

Effect of plasma microfields on the gain of hydrogen-like ions with photoresonant pumping

P. D. Gasparyan, V. M. Gerasimov, A. N. Starostin, and A. E. Suvorov

Troitsk Institute of Innovative and Thermonuclear Research, 142092 Troitsk, Moscow Region, Russia
(Submitted 14 December 1993)

Zh. Eksp. Teor. Fiz. **105**, 1593–1605 (June 1994)

A model is constructed and used to study the effect of Stark microfields on the gain of a weak signal in a plasma of hydrogen-like ions with photoresonant pumping. The accuracy of the radiative-collisional model as an approximation for describing the kinetics of multicharged ions in a plasma is studied, taking into account the effect of electric microfields on both the spectral line shape and on the dynamics of the atomic system, using the density matrix formalism. Results are reported from numerical calculations of the spectral response of a weak signal at the 4→3 and 3→2 transitions of hydrogen-like nickel ions.

1. INTRODUCTION

One of the most important problems in laser physics is that of creating x-ray lasers. If we consider quantum mechanical systems with discrete levels as candidates for the working medium of an x-ray laser it is easy to see that x-ray lasing corresponds to an energy typical of intraatomic transitions or transitions between the excited states of multicharged ions. The first estimates (1964) of the power needed in pumps in order to achieve inversion in such systems revealed that the power is extremely high,¹ and this consideration required experimental and theoretical studies of x-ray lasers for a long time. The required power level estimated by Prokhorov,¹ $I_{\max} \approx 10^{17} - 10^{18}$ W/cm², corresponds to a thermal radiation source with a temperature of $T \approx 1-3$ keV. The only source of radiation at this temperature under terrestrial conditions is a nuclear or thermonuclear explosion. And to be sure, the announcements of experimental studies of x-ray lasers which appeared in 1981 (Ref. 2) confirmed that an x-ray laser had been developed with pumping from radiation produced by a nuclear or thermonuclear explosion. Although the basic data about x-ray lasers of this type have not yet appeared in the open literature, those publications which are available^{3,4} confirm that the x-ray laser was pumped by a nuclear explosion with a yield of 20–100 kton, which easily suffices to provide a pump with the strength estimated in Ref. 1.

Substantial progress in the late 1970s and early 1980s in creating laboratory sources of high power, up to $10^{14}-10^{16}$ W, is associated with large-scale studies of controlled thermonuclear fusion (ion- and laser-driven inertial confinement fusion) permitted the development of a program for laboratory studies of x-ray lasers.⁵ To date several designs have been proposed for laboratory x-ray lasers operating in the wavelength range from 50 to 300 Å (Ref. 5). The greatest progress in laboratory studies has been achieved with recombination x-ray lasers utilizing [H]- and [Li]-like ion transitions in an expanding plasma containing multicharged ions, and collisional pumping at transitions of [Ne]-like ions. (For a review of the results see, e.g., Refs.

5 and 6.) On the other hand, in theoretical investigations most of the emphasis has been placed in x-ray designs based on the use of the radiative properties of a multicharged plasma to produce inversion.

Of these designs the most important are those with resonant photopumping (analogous to designs with optical pumping in lasers operating in the visible wave band), originally suggested in order to demonstrate x-ray lasing⁷⁻¹⁰ and a number of new resonant and hybrid schemes.¹¹ Most of the interest in such schemes arises from the prospect of higher gains in the x-ray radiation, extension further into the short-wavelength region, and reduction in the divergence of the laser radiation.¹¹ It should be noted that designs using photopumping obviously require more powerful pump sources for their operation than do recombination and collisional designs. Consequently, the prospects in laboratory studies depend on making progress in creating high-power sources, for which purpose those such as nuclear explosions are naturally irrelevant. The prospect for creating the most powerful laboratory sources for x-ray laser pumping is associated with the development of new devices for RCF with energy of up to 1 MJ and with attempts to reduce the pulse length of the pump to 1 ps.

To date there have been no demonstrations of designs for laboratory x-ray lasers with resonant pumping in the soft x-ray range. The shortest wavelength at which significant gain has been measured with resonant pumping is 2163 Å in [Be]-like carbon.¹² It is possible that this is related to a number of theoretical problems which have not been studied adequately to permit reliable calculation of x-ray lasing in the short-wavelength range. We note the following fundamental problems, which are important for theoretical and computational modeling of x-ray lasers with resonant pumping: the need to calculate the intensity of the resonant pump radiation in the nonequilibrium plasma of radiation converters, and estimating the accuracy of the kinetics of excited-state populations of multicharged ions in the balance equations for a high-density high-temperature plasma.

These two problems are interrelated and have been investigated intensively in connection with studies of a

large number of goals of importance to the physics of high energy densities. These objectives include the laboratory plasma in high-power physics experiments in thermonuclear studies (pinches, tokomaks, laser targets), space, coronal, and photospheric plasma from astrophysical radiation sources, etc. But the finest details in the behavior of a multicharge plasma are of importance for x-ray lasers, since the generation of x-ray laser radiation is a sensitive indicator of nonequilibrium kinetic processes.

X-ray laser theory has a number of questions in common with ordinary glass lasers in the visible range. The differences in the kinetics of x-ray lasers from that in optical lasers are a consequence of the important role of radiative processes in a multicharged ion plasma relative to the collisional processes, the important effect of plasma microfields and their statistics on the spontaneous emission spectra of the ions and the cross sections for induced processes, and relativistic effects on the energetic structure of the emitters. In particular, these properties require more careful studies of the conditions under which it is appropriate to use the approximation of total frequency redistribution in forming the resonant pump spectrum. This approximation is usually applicable in the analysis of radiative processes in a plasma (see, e.g., Refs. 13 and 14) and treatment of frequency redistribution effects for some resonant lines when microfields are present.¹⁵

As a specific example we consider the simplest resonant pump design,⁶ in which inversion is produced at the 4→3 and 3→2 transitions between excited states of [H]-like ions, and L_α or [He]_α radiation is used for the pump. A considerable number of resonant pairs for this scheme are given in Ref. 16. There calculations of the population inversion and the gain coefficients K_{3→2}, K_{4→3} in [H]-like Cl ions are reported. The pumping is done by L_α and He_α K radiation in a slab laser target with parameters ρ_{Cl,K}≈0.006 g/cm³, T_{e,i}≈2 keV, ΔR_{Cl}=10 μm, and ΔR_K=500 μm. This design does not use external irradiation of the targets; the resonant photons are produced through radiative decay of excited [H]- and [He]-like K ions, whose states are populated in relatively slow collisional processes.⁶ Note that when external irradiation of the target is used by a source of nonequilibrium hard radiation with a continuous spectrum, e.g., that treated in Ref. 17 (Sects. 2.4.2 and 4.4) in order to produce a radiatively supercooled plasma through bulk ionization, the resonant pump radiation can act through radiative processes that are faster than collisional ones. We have in mind the process of photon subdivision, familiar in astrophysics (the Rosseland theorem, Ref. 13, Ch. 5), in which the resonant radiation is produced in the plasma by virtue of purely radiative processes. The efficiency of this mechanism increases as a function of the ion charge state Z, and it is natural to use this mechanism for producing resonant radiation when an appropriate source of external radiation is present (e.g., a thermonuclear explosion).

We now direct our attention to the kinetics by which a population inversion is produced in hydrogen-like Cl ions for the target of Ref. 16. When the n=3 level is resonantly pumped and lasing occurs at the 3→2 transitions the fol-

lowing problem arises. If we disregard collisional processes, then it is impossible to create an inversion in the 3→2 transition through radiative pumping of the n=3 level in the 1→3 (L_β) transition and radiative depopulation of the n=2 level because of the angular-momentum selection rules: in the succession of transitions 1s→3p (pumping) and 3p→2s (the lasing transition), in the dipole approximation the 2s level is metastable with respect to radiative decay. For “cyclic” generation in the dipole-allowed transitions a four-level scheme is necessary, i.e., either radiative pumping of the n=4 level or the inclusion of collisional “repumping” (mixing) of excitations with respect to the suborbitals of the states with n=3 or n=2. In the radiation–collision model of plasma kinetics this mixing of states results from relatively slow electron collisions and collisions with ions. It can be shown that for ion states which are nondegenerate in l, when the nearest levels to the specified ones are separated in energy by a considerable amount, collisions with ions are adiabatic and under many conditions of practical interest give rise only to elastic broadening of the line, describable by collision theory. Then, because there is a small parameter (the gas parameter, i.e., the number of particles in the Weisskopf sphere) in the impulsive approximation it is possible to derive in a fairly rigorous fashion the collision integral and the quantum kinetic equation for the atomic density matrix and the conditions for the applicability of the radiative–collisional model.^{18,19} The impulsive approximation is applicable for describing collisions with electrons for essentially all parameters of the multicharged x-ray plasma. However, in the case of states that are degenerate in l, such as hydrogen-like ions, the conditions for the applicability of the impulsive approximation to describe collisions with ions are frequently violated (for example, in the K–Cl vapor x-ray laser of Ref. 16). For states that are degenerate in l the Stark effect is linear in the field, so that there are a relatively large number of particles in the Weisskopf sphere and “collisions” with ions have a multiple character. In line-broadening theory this case is investigated by using the statistical (or more precisely, the static) approach,²⁰ which contrasts with the impulse approximation. Here the ion radiation spectrum is initially calculated for constant plasma microfields, and then the spectrum is averaged over the probability of realizing the fields in a Gibbs ensemble. Corrections for the time variation of the field are taken into account using perturbation theory.²⁰

The same idea can be used to analyze the effect of ion collisions on the kinetics of degenerate-state “mixing” in a multicharged x-ray laser plasma and the gain of the laser radiation in transitions between degenerate states. Here the effects of the time variation of the fluctuating low-frequency plasma microfields can be taken into account through the appropriate generalization of the theory, either postulating stochastic properties for the microfields or using numerical techniques to treat “ion dynamics,” as was done, e.g., in Ref. 21 for the kinetic theory of Stark broadening.

In the present work the atomic density matrix method is applied in the static approximation in the microfields to

solve the problem of finding the spectral gain (absorption) coefficient for a weak signal in transitions between the $4 \rightarrow 3$ and $3 \rightarrow 2$ states of hydrogen-like nickel ions over a broad range of plasma densities. Nickel has been chosen as a typical representative of plasmas with intermediate nuclear charges $Z \sim 30$, although no simple vapors are known specifically for it which could be used in resonant photopumping. The amplifying medium is assumed to be optically thin.¹⁾ The solution is derived for a constant microfield and then averaged over the microfield distribution function. This approach enables us to treat nonlinear interference effects¹⁸ associated with the interaction of the plasma microfields and the gain coefficient resulting from coherent excitation of degenerate suborbitals in induced transitions (see also Refs. 15 and 21). Some aspects of the processes considered here, associated with the change in the lifetime of long-lived states due to their Stark mixing with short-lived states, are discussed conceptually in Ref. 22.

The effects of "field" mixing of states and the influence of ion collisions on the line profiles are important in connection with optimizing the lasing conditions in the active medium of an x-ray laser. This is associated primarily with the choice of the working plasma density, since at densities that are too low the gain of the laser radiation is small, while when the density is too high the population inversion is weak due to thermalization of the states. The use of the radiative-collisional model for lasing in transitions of helium-like ions to "optimize" the density has been studied numerically in Ref. 10. As will be seen from the results of the present work, for lasing in transitions of hydrogen-like ions, for which "ion" collisions are strong because of the degeneracy of the states in l , optimization of the density of the medium in terms of the gain should take into account the effect of the plasma microfields. Since relaxation of the populations (the diagonal elements of the density matrix) and of the polarizations (the nondiagonal elements) are not separate processes, the density cannot be optimized by means of calculations using the relaxation-collisional model, generally speaking, and more precise calculations using the atomic density matrix method are required.

Going beyond the bounds of the radiation-collisional model significantly complicates kinetic calculations of x-ray lasers due to the increase in the size of the system of kinetic equations to be solved, as well as the need to take into account the ion dynamics of the microfields. These complications increase in calculations of x-ray lasers in the saturated regime when the effect of lasing on the level populations is important. Hence it is desirable to derive simplified kinetic models in which the effect of the microfields is included only for those transitions where it is most important, while the majority of transitions are described in the radiation-collisional approximation. Another fundamental problem involves describing reabsorption of resonant radiation in a plasma of multicharged ions when the effect of the plasma microfields on the photon frequency distribution function is taken into account (see, e.g., Ref. 15).

The problem of the amplification of a weak signal in the $ns_{1/2} \rightarrow n'p_{1/2}$ transition in hydrogen-like atoms, which

we solved in 1985–1986 using the atomic density matrix method, was published in Ref. 23.

2. THEORETICAL MODEL FOR DESCRIBING THE KINETICS OF AN ATOMIC SUBSYSTEM IN AN EXTERNAL ELECTROMAGNETIC FIELD

The complete description of the behavior of a system of hydrogen-like ions in a plasma requires the solution of kinetic equations for the possible processes of ionization, recombination, and radiative and collisional transitions between levels in which ion interactions with the plasma microfield are taken into account, along with the effect of pumping on the particular level. As shown by a comparison of the results of calculations of the Ly_α line profiles carried out, e.g., for Ar XVIII with electron densities $N_e < 10^{23} \text{ cm}^{-3}$, the effects associated with ion dynamics do not reveal differences from the calculations in the static approximation.²¹ As the nuclear charge increases the relaxation rate of the atomic subsystem increases in proportion to Z^4 , and the time dependence of the microfields in this density range becomes even less important for the hydrogen-like nickel ion. In this connection we can assume that the plasma microfield \mathbf{E} varies slowly, and write down the time-independent equations for the density matrix of the hydrogen-like ions, $\hat{\rho}_0 = \rho_{n_1 l_1 m_1 n_2 l_2 m_2} = \rho_{12}$:

$$\frac{i}{\hbar} [\hat{H} + \mathbf{E}\hat{\mathbf{d}}, \hat{\rho}_0] = -\Gamma(\hat{\rho}_0) + S(\hat{\rho}_0) + \hat{Q}. \quad (1)$$

In this equation \hat{H} is the diagonal energy matrix of the hydrogen-like ion, taking into account the fine structure and the Lamb shift.²⁴ The relaxation operator $\Gamma(\hat{\rho}_0)_{12} = 0.5(\gamma_1 + \gamma_2)\rho_{12}$ includes spontaneous decay, the processes of photo- and collisional ionization, and inelastic collisions with electrons. The matrix of the dipole moment operator $\hat{\mathbf{d}}$ and the photoprocess rates are calculated from the exact hydrogen formulas,²⁵ the collisional ionization from the Lotz formula,¹⁹ the inelastic collisions that give rise to the change in the principal quantum number n according to the Van Regemorter formula,¹⁹ and the processes that lead to transitions between states associated with the same level using the formulas derived from perturbation theory which are widely employed in calculations of the line broadening due to electron impact.¹⁹ The input recombination term \hat{Q} is a diagonal operator and includes the processes inverse to these ionization channels, referred to a single completely ionized atom. The input operator $S(\hat{\rho}_0)_{12} = \sum' S_{12 \ 1'2'} \rho_{1'2'}$, includes transitions into this state from other states due to the action of pumping and radiative and collisional transitions between states. The contribution of the latter two mechanisms can be represented in the form

$$S_{12 \ 1'2'} = (S' + S^c) \mathbf{d}_{11'} \mathbf{d}_{22'}^*. \quad (2)$$

The coefficient for radiative transitions is equal to

$$S' = \frac{4}{3\hbar} \left(\frac{\omega_{n'n}}{c} \right)^3, \quad n' > n. \quad (3)$$

For collisional transitions in which the principal quantum number does not change the coefficient is equal to

TABLE I.

3→2 Transition	Transition energies, eV	4→3 Transition	Transition energies, eV
$3s_{1/2} \rightarrow 2p_{3/2}$	-5.24	$4p_{1/2} \rightarrow 3d_{3/2}$	-1.53
$3d_{3/2} \rightarrow 2p_{3/2}$	2.80	$4s_{1/2} \rightarrow 3p_{3/2}$	-1.45
$3d_{5/2} \rightarrow 2p_{3/2}$	5.56	$4p_{3/2} \rightarrow 3d_{5/2}$	-0.80
$3p_{1/2} \rightarrow 2s_{1/2}$	21.8	$4f_{5/2} \rightarrow 3d_{5/2}$	0.356
$3s_{1/2} \rightarrow 2p_{1/2}$	22.7	$4f_{7/2} \rightarrow 3d_{5/2}$	0.938
$3p_{3/2} \rightarrow 2s_{1/2}$	30.0	$4d_{3/2} \rightarrow 3p_{3/2}$	1.94
$3d_{3/2} \rightarrow 2p_{1/2}$	30.7	$4p_{3/2} \rightarrow 3d_{3/2}$	1.96
		$4d_{5/2} \rightarrow 3p_{3/2}$	3.10
		$4f_{5/2} \rightarrow 3d_{3/2}$	3.11
		$4p_{1/2} \rightarrow 3s_{1/2}$	6.51
		$4s_{1/2} \rightarrow 3p_{1/2}$	6.82
		$4p_{3/2} \rightarrow 3s_{1/2}$	10.0
		$4d_{3/2} \rightarrow 3p_{1/2}$	10.2

$$S^c = \frac{8N_e}{3} \left(\frac{e}{\hbar} \right)^2 \left(\frac{2\pi m_e}{T_e} \right)^{1/2} \ln \frac{R_D}{r_{\min}}, \quad (4)$$

where R_D is the Debye radius and r_{\min} is calculated as the smaller of the radius of an electron orbit, the radius of the Weisskopf sphere, the wavelength of a perturbed electron, and the distance at which the Coulomb interaction energy with the nucleus is equal to the electron thermal energy. The rates according to Van Regemorter for collisional transitions between levels with different principal quantum numbers are proportional to the square of the dipole moment, so we decided it was sensible to use Eq. (2) for them as well. The coefficient was chosen so that summation over all final states and averaging over all initial states yielded the Van Regemorter formula. The pumping action of external radiation into the given level was taken into account by the input terms from the ground state into the p states with a proportionality coefficient $\gamma \bar{n}/2$, where γ is the rate of spontaneous decay for the corresponding ps transition and the occupation number \bar{n} or the pump characterizes its intensity.

Since all processes other than interaction with the electric field are isotropic and the field mixes only states with the same principal quantum number n , if we introduce a quantization axis parallel to the plasma microfield E the density matrix will be diagonal in n and in the projection m

of the angular momentum, i.e., we obtain a system of equations for $\rho_{n_j l_1 m n_j l_2 m}$. Using the elementary properties of the $3j$ symbols and the parity selection rules, we can show that the density matrix obtained from solving Eqs. (1) satisfies the relation

$$\rho_{n_j l_1 m n_j l_2 m} = (-1)^{j_1 - j_2 - l_1 + l_2} \rho_{n_j l_1 - m n_j l_2 - m}. \quad (5)$$

If we recall that $\rho_{12} = (\rho_{21})^*$ holds, then the density matrix of each level n is determined by $n(4n^2 - 1)/3$ real quantities. Thus, to describe four levels we need $1 + 10 + 35 + 84 = 130$ quantities.

Detailed calculations show that for levels with $n > 4$ electron collisions mix states with different angular momenta quite well, so that we treat these levels as hydrogen-like with uniform occupation of states having the same principal quantum number, and we describe them in terms of their populations rather than using the density matrix.

In order to calculate the gain we treat the interaction of a hydrogen-like ion with a test monochromatic wave $E_\omega \exp(-i\omega t) + c.c.$, whose frequency is resonant with the radiative transition $n_1 - n_2$. In the first order of perturbation theory a density matrix appears which is nondiagonal in the principal quantum number. By expanding the vector E_ω in spherical harmonics we can represent it in the form

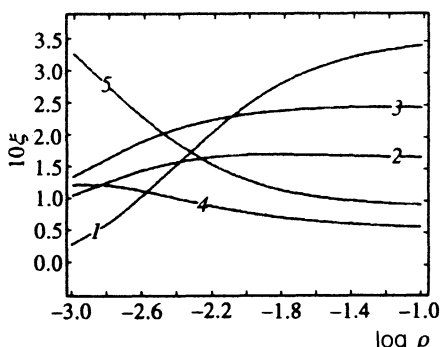


FIG. 1. Normalized total gain $\xi = g\gamma\Delta n / \Sigma g\gamma\Delta n$. 1— $4f_{7/2} \rightarrow 3d_{5/2}$, 2— $4d_{5/2} \rightarrow 3p_{3/2}$, 3— $4f_{5/2} \rightarrow 3d_{3/2}$, 4— $4p_{3/2} \rightarrow 3s_{1/2}$, 5— $4d_{3/2} \rightarrow 3p_{1/2}$.

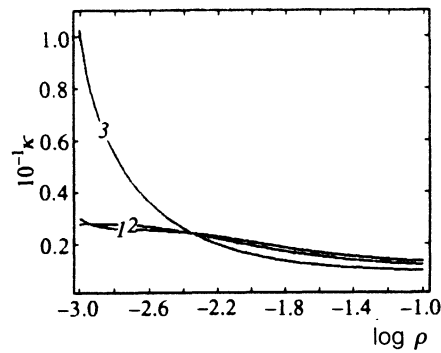


FIG. 2. Ratio of the average total gain to the gain with zero field for the lines 1— $\lambda = 23.87 \text{ \AA}$, 2— $\lambda = 23.77 \text{ \AA}$, 3— $\lambda = 23.45 \text{ \AA}$.

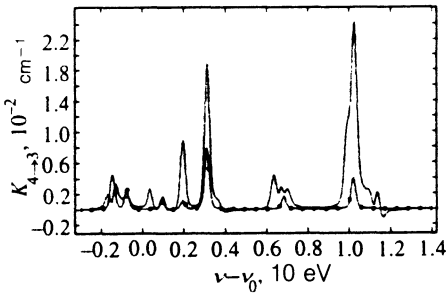


FIG. 3. Gain at the 4→3 transition ($\rho=0.001 \text{ g/cm}^3$). The solid traces correspond to the calculation in which the plasma microfields are completely included; the points correspond to the calculation of the spectrum without microfields.

$\hat{\rho}_1 = \exp(-i\omega t) \Sigma_q (E_\omega^q)^* \hat{\rho}^q$. The equation for the expansion coefficients of the density matrix is similar to (1):

$$\frac{i}{\hbar} [\hat{H} + \hat{E}_d, \hat{\rho}^q] - i\omega \hat{\rho}^q = -\Gamma(\hat{\rho}^q) + S(\hat{\rho}^q) - \frac{i}{\hbar} [d^q, \hat{\rho}_0]. \quad (6)$$

Since $\hat{\rho}_0$ is diagonal in m , the matrix ρ_{12}^q is nonvanishing if $m_2 = m_1 + q$ holds. Moreover, in analogy with (5) we have

$$\rho_{n_1 j_1 l_1 m_1 n_2 j_2 l_2 m_2}^q = (-1)^{j_1 - j_2 - l_1 + l_2} \rho_{n_1 j_1 l_1 - m_1 n_2 j_2 l_2 - m_2}^{-q}. \quad (7)$$

For $q=0$ this reduces the number of independent variables by a factor of two, and $\hat{\rho}^{-1}$ is uniquely expressed in terms of $\hat{\rho}^1$. For the 3→2 transition the density matrix has 36 independent quantities for $q=0$ and 60 for $q=1$. For the 4→3 transition the corresponding numbers are 106 and 192.

After we solve Eqs. (1) and (6) for different values of the plasma microfield we can average the density matrix over the Holtsmark distribution. The average in the direction of the microfield is equivalent to averaging with respect to the direction of E_ω . The gain of the emission from the $n_1 - n_2$ transition can be found from the formula

$$K(\omega) = \frac{4\pi}{3c} N_i \operatorname{Re} \sum_{q,1,2} (d_{12}^q)^* \hat{\rho}_{12}^q. \quad (8)$$

Averaging (8) over the distribution of Doppler shifts kv of the frequency we obtain the final expression for the gain.

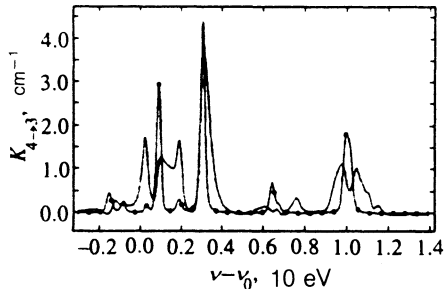


FIG. 4. Gain at the 4→3 transition ($\rho=0.01 \text{ g/cm}^3$). The plotting conventions are the same as in Fig. 3.

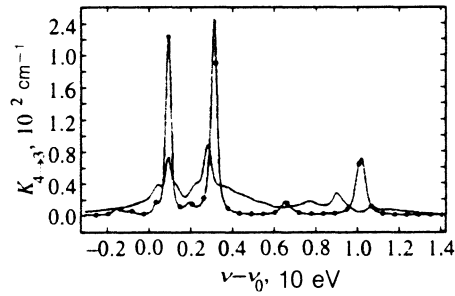


FIG. 5. Gain at the 4→3 transition ($\rho=0.1 \text{ g/cm}^3$). The plotting conventions are the same as in Fig. 3.

3. RESULTS OF CALCULATING THE SPECTRAL RESPONSE OF A WEAK SIGNAL IN THE 4→3 AND 3→2 TRANSITIONS OF HYDROGEN-LIKE NICKEL IONS

To make it easier to identify the lines, in the Table I we present the energy shifts of the transitions of hydrogen-like nickel ions used in the calculations. These have been obtained from the nonrelativistic values.²⁴

We begin by attempting to distinguish the effect of the field on the spectrum in terms of the change in occupations from the effective broadening. Integration of the spectrum with respect to frequency yields the relation

$$\int K(\omega) d\omega = N_i \left(\frac{\pi c}{\omega} \right)^2 \sum_{1,2} g_1 \gamma_{12} (n_1 - n_2), \quad (9)$$

where $n = N/g$ is the occupation of a single suborbital. Since individual fine-structure lines in the spectrum are more or less identified (at least when the densities are not too high so that electron collisions do not cause the fields to affect populations), we can use the magnitude of the terms in Eq. (9) as a global measure of the strengths of the individual lines, and from the variation of these magnitudes in the electric field we can infer how important it is to include the fields in the first stage of the solution, evaluation of the density matrix.

In the calculations the ionic composition of the plasma, the electron temperature, and the occupation number \bar{n} of the pump were specified.

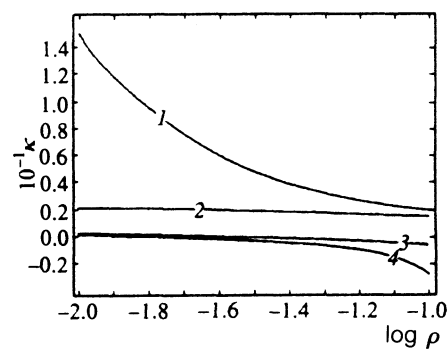


FIG. 6. Ratio of the average total gain to the gain with zero field for the lines 1— $\lambda = 8.353 \text{ \AA}$, 2— $\lambda = 8.337 \text{ \AA}$, 3— $\lambda = 8.245 \text{ \AA}$, 4— $\lambda = 8.199 \text{ \AA}$.

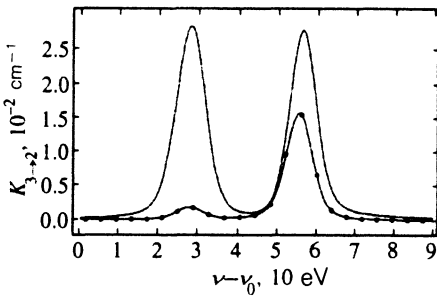


FIG. 7. Gain for the lines $\lambda=8.353 \text{ \AA}$ and $\lambda=8.337 \text{ \AA}$ ($\rho=0.01 \text{ g/cm}^3$). The plotting conventions are the same as in Fig. 3.

We start by considering the case of pumping into level 4 ($\bar{n}=0.03$, $T_e=1.8$, $0.001 < \rho < 0.1$). The density dependence of the overall gain, normalized with respect to the full sum, is shown in Fig. 1 for the five strongest transitions. The contribution of the other transitions was less than 25%.

These five transitions form the three lines which are most conspicuous in the spectrum: the $4f_{7/2} \rightarrow 3d_{5/2}$ transition, the line which is found in the figures near 0.94 eV (according to Ericson²⁴ $\lambda=23.87 \text{ \AA}$); the $4d_{5/2} \rightarrow 3p_{3/2}$ and $4f_{5/2} \rightarrow 3d_{3/2}$ transitions, corresponding to the 3.1 eV line ($\lambda=23.77 \text{ \AA}$)²; and the $4p_{3/2} \rightarrow 3s_{1/2}$ and $4d_{3/2} \rightarrow 3p_{1/2}$ transitions, corresponding to the 10 eV line ($\lambda=23.45 \text{ \AA}$). Figure 2 shows the effect of the electric field on the intensity of these lines for different densities. At high densities the effect of the field is neutralized by electron mixing, and in the beginning and the middle of this density range for the 23.87 Å and 23.77 Å lines the effect increases by a factor of two, while for the 23.45 Å line it increases by a factor of ten. This circumstance is related to the strong effect of the field on the occupation of the $3s_{1/2}$ level. It is noteworthy that including the field in the stage of the calculation where the populations are determined under these conditions increases the gain.

The above analysis does not include the effects of the nondiagonal elements of the density matrix, specifically the broadening by the field, which is treated in the stage where the spectrum is calculated. Both of these change the shape of a line while retaining its total magnitude. Distinguishing one effect from the other is unlikely to be simple, although the nondiagonal elements should probably not play a major

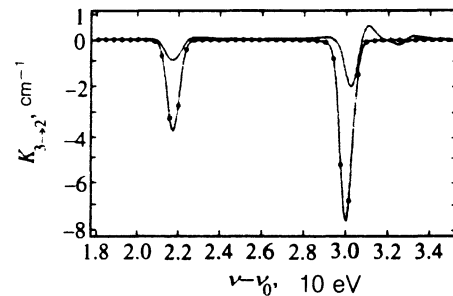


FIG. 9. Gain for the lines $\lambda=8.245 \text{ \AA}$ and $\lambda=8.199 \text{ \AA}$ ($\rho=0.01 \text{ g/cm}^3$). The plotting conventions are the same as in Fig. 3.

role. Comparison of the spectrum with complete treatment of the plasma field (solid trace) and the spectrum without the field (trace marked with filled circles) is made for various densities in Figs. 3–5. At low densities, when broadening by the field does not play a major role, the ratio of the maxima of the lines corresponds to the values in Figs. 1 and 2. At intermediate densities the effects of broadening and the change in the field through population of the levels can act in either direction, and for the 23.77 Å line the maxima obtained including the field and without it are approximately the same, although the line is significantly broader in the former instance. For the other two lines the effect from broadening is considerably greater than the effect of the change in populations. At high densities only the broadening effect is actually manifested, and it is very large.

Now we will consider the case of pumping into level 3 ($\bar{n}=0.027$, $T_e=1.8$, $0.01 < \rho < 0.1$).³⁾ In the spectra four lines are clearly delineated: 2.8 eV (the $3d_{3/2} \rightarrow 2p_{3/2}$ transition, $\lambda=8.353 \text{ \AA}$); 5.6 eV (the $3d_{5/2} \rightarrow 2p_{3/2}$ transition, $\lambda=8.337 \text{ \AA}$); 22 eV (the $3p_{1/2} \rightarrow 2s_{1/2}$ and $3s_{1/2} \rightarrow 2p_{1/2}$ transitions, $\lambda=8.245 \text{ \AA}$); and 30 eV (the $3p_{3/2} \rightarrow 2s_{1/2}$ and $3d_{3/2} \rightarrow 2p_{1/2}$ transitions, $\lambda=8.199 \text{ \AA}$). The $3s_{1/2} \rightarrow 2p_{3/2}$ transition is barely detectable. Figure 6 shows the extent to which including the effect of the field changes the total strength of these lines.

The most conspicuous feature of these results is the very strong field strength dependence of the 8.353 Å line. The transition probability for this line is low, so under ordinary circumstances when the populations of the $3d_{3/2}$ and $3d_{5/2}$ levels are comparable, this line is very weak; this

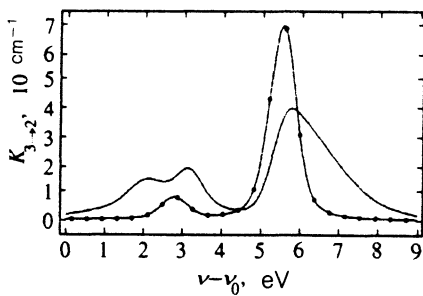


FIG. 8. Gain for the lines $\lambda=8.353 \text{ \AA}$ and $\lambda=8.337 \text{ \AA}$ ($\rho=0.1 \text{ g/cm}^3$). The plotting conventions are the same as in Fig. 3.

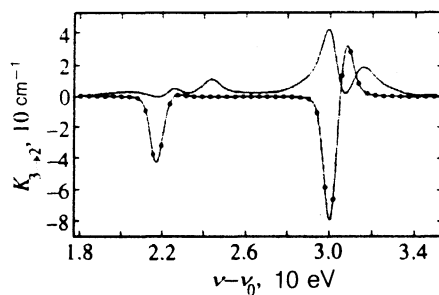


FIG. 10. Gain for the lines $\lambda=8.245 \text{ \AA}$ and $\lambda=8.199 \text{ \AA}$ ($\rho=0.1 \text{ g/cm}^3$). The plotting conventions are the same as in Fig. 3.

is clearly seen in Fig. 7 for the spectrum without inclusion of the field. Mixing of the $3p_{3/2}$ level, which is populated by optical pumping, and the $3d_{3/2}$ level in the electric field increases the population of the latter by about an order of magnitude, which leads to equilibration of the intensities of the 8.353 and 8.337 Å lines. As the density increases this effect drops due to mixing by electron collisions (Fig. 8).

At low densities the 8.245 and 8.199 Å lines exhibit absorption due to the high population of the $2s_{1/2}$ level (Fig. 9). When the effect of the electric field is not treated, since this level is metastable the high population is maintained, so that the 8.245 and 8.199 Å lines are absorbing at all densities. Interaction with the field reduces the occupation of the $2s_{1/2}$ level, and at high densities (Fig. 10) both lines exhibit gains. In accordance with this the ratio of the intensities when the effect of the field is omitted and when it is included for these lines, shown in Fig. 6, becomes negative with increasing density.

4. CONCLUSION

In this work we have used the density matrix technique in the static approximation in the plasma microfield to solve the problem of determining the spectral gain of a weak signal in transitions between the $4 \rightarrow 3$ and $3 \rightarrow 2$ states of hydrogen-like nickel ions. This approach enables us to include the effect of nonlinear interference phenomena¹⁸ in the action of the plasma microfields on the gain, which arise due to coherent excitation of degenerate suborbitals in induced transitions.

From the results we have presented it follows that in order to produce lasing in hydrogen-like ions the density of the working medium should be optimized with respect to the gain by taking into account the plasma microfields. Optimization of the density to calculations using the collisional-radiative model, generally speaking, is inappropriate. It is necessary to use the density matrix method in calculations.

One of the present authors (A. E. Suvorov) is grateful to the Soros fund for providing a grant from the American Physical Society (1993).

¹⁸For densities of interest to us with $\rho < 0.1 \text{ g/cm}^3$, this corresponds to

typical transverse dimensions of the amplifying medium $< 100 \mu\text{m}$ for the resonant Ly_α line, and $< 1 \mu\text{m}$ for the H_α line.

- ²⁾The wavelengths of doublet lines are given in terms of the long-wavelength component.
- ³⁾The range of densities is diminished in comparison with the previous case, since for densities $\sim 10^{-3}$ only absorption lines from the $2s_{1/2}$ level, which at these densities depends weakly on the field, can be discerned.

- ¹A. M. Prokhorov, "Nobel Prize Lecture," *Science* **149**, 828 (1965).
- ²C. A. Robinson, AV&ST, **114**, 25–27 (1981).
- ³"Report to the American Physical Society of the Study Group on Science and Technology of Directed Energy Weapons: Executive Summary and Major Conclusions," *Physics Today* **40**(5), S3–S15 (May 1987); Complete report published in *Rev. Mod. Phys.* **59**(3), pp. II-S1–S202 (July 1987).
- ⁴W. J. Broad, *Teller's War*, Simon & Schuster (1992).
- ⁵Ch. H. Skinner, *Phys. Fluids* **B3**, 242 (1991).
- ⁶R. C. Elton, *X-Ray Lasers*, Academic Press (1991).
- ⁷A. V. Vinogradov, I. I. Sobel'man, and E. A. Yukov, *Kvantovaya Elektron.* **2**, 167 (1975) [Sov. J. Quantum Electron. **5**, 103 (1975)].
- ⁸B. A. Norton and N. J. Peacock, *J. Phys.* **B8**, 989 (1975).
- ⁹V. A. Bhagavatula, *J. Phys.* **47**, 4535 (1976).
- ¹⁰W. E. Alley, G. Chapline, P. Kunasz, and J. C. Weisheit, *JQSRT* **27**, 257 (1982).
- ¹¹J. Nilsen, *Izv. Akad. Nauk SSSR* **55**, 782 (1991).
- ¹²W. Oi and M. Krishnan, *Phys. Rev. Lett.* **59**, 2051 (1987).
- ¹³D. Mikhalas, *Stellar Atmospheres*, Freeman, San Francisco (1970).
- ¹⁴L. M. Biberman, V. S. Vorob'yev, and I. T. Yakubov, *Kinetics of Non-equilibrium Low-Temperature Plasmas*, Consultants Bureau, New York (1982).
- ¹⁵A. V. Anufrienko, A. L. Godunov, A. V. Demura *et al.*, *Zh. Tekh. Fiz.* **98**, 1304 (1990); [Sov. Phys. Tech. Phys. **71**, 728 (1990)].
- ¹⁶J. Nilsen, J. Scofiled, and E. Chandler, *Appl. Optics* **31**, 4950 (1992).
- ¹⁷V. I. Derzhiev, A. G. Zhidkov, and S. I. Yakovlenko, *Ion Emission in Dense Nonequilibrium Plasmas* [in Russian], Energoatomizdat, Moscow (1986).
- ¹⁸S. G. Rautian, G. I. Smirnov, A. M. Shalagin, *Nonlinear Resonances in Atomic and Molecular Spectra* [in Russian], Nauka, Novosibirsk (1979).
- ¹⁹L. A. Vainshtein, I. I. Sobel'man, and E. A. Yukov, *Excitation of Atoms and Broadening of Spectral Lines*, Springer, New York (1981).
- ²⁰V. I. Kogan, V. S. Lisitsa, and G. V. Sholin, in *Reviews of Plasma Physics*, Vol. 13, B. B. Kadomtsev (ed.), Consultants Bureau, New York (1987).
- ²¹A. V. Anufrienko, A. E. Bulyshev, A. L. Godunov *et al.*, *Zh. Eksp. Teor. Fiz.* **103**, 417 (1993) [Sov. Phys. JETP **76**, 219 (1993)].
- ²²V. I. Kogan, V. S. Lisitsa, and A. D. Selidovkin, *Zh. Eksp. Teor. Fiz.* **65**, 152 (1973) [Sov. Phys. JETP **38**, 75 (1974)].
- ²³P. D. Gasparyan and V. M. Gerasimov, VANT No. 1 (1993).
- ²⁴Glen W. Ericson, *J. Phys. Chem. Ref. Data* **6**, 831 (1977).
- ²⁵V. B. Berestetskii, E. M. Lifshitz, and L. P. Pitaevskii, *Quantum Electrodynamics*, Pergamon, Oxford (1982).

Translated by David L. Book